Chapter 6

Morphogenesis of Cement Hydrate: From Natural C-S-H to Synthetic C-S-H

Rouzbeh Shahsavari and Sung Hoon Hwang

Additional information is available at the end of the chapter

http://dx.doi.org/10.5772/intechopen.77723

Abstract

Triggered by the recent advance in materials synthesis and characterization techniques, there has been an increasing interest in manipulating properties of calcium silicate hydrates (C-S-H), which constitute the fundamental, strength-responsible building blocks of concretes. Concretes are the indispensable constituents of today's modern infrastructures and simultaneously the most widely used synthetic material on the planet. Despite the widespread impact and high societal values, the production of their major binder component, Portland cement (PC), is the major culprit for global warming since it contributes to 5–10% carbon dioxide emission worldwide. Consequently, enhancing the ultimate strength and durability of concretes by tuning structural, compositional and mechanical properties of their basic building units and assembling them via bottom-up engineering is one of the key strategies to mitigate the aforesaid concerns. This is simply because the longer the concretes last, the less production of PC would incur. Furthermore, the current role of C-S-H in industry is not only confined to the context of construction materials but to diverse sectors of industry including drug delivery, CO_2 sorbent and materials for bone replacement. This wide scope of potential applications can be ascribed to the high versatility regarding tunable structural properties such as porosity, size and morphology, all of which can be fine-tuned during the synthetic procedure. Among the listed properties, understanding and gaining control over morphological factors of C-S-H is particularly important since they are directly associated with their functional roles. C-S-H with various morphologies can be produced by altering key experimental conditions, which encompass types of synthetic procedure, precursor types such as different calcium and silicate sources and types of additives. This chapter discusses a variety of morphologies of C-S-H acquired in multiple environments. The latter include the hydration of PC or PC-blends containing supplementary materials such as slag, synthetic C-S-H produced using silica-lime reactions and crystalline CSH synthesized using hydrothermal treatment. At the end, the chapter will provide a complete review on the current range of morphologies for calcium silicate hydrate.

Keywords: cement hydrate, shape-controlled synthesis, cubic cement, calcium silicate hydrate

1. Morphology of C-S-H observed during the hydration of PC or PC-based blend

Before reviewing the morphology of naturally formed, semicrystalline C-S-H acquired during the hydration of PC, it is necessary to review its nucleation and growth mechanism during the hydration process. Despite the decadelong efforts, the complete picture for the mechanism of C-S-H formation during the hydration of cement is yet to be acquired, and several nucleation, growth and structural models have been proposed [1, 2]. The consensus is that the initial stage is comprised of dissolution of cement phases such as tricalcium silicate (C_3S) and dicalcium silicate (C_2S), releasing calcium, hydroxide, and silicate ions [3, 4]. Jennings et al. studied morphological development of hydrating C_3S, one of the major phases of cement, using the combination of multiple electron microscopic techniques, transmission electron microscopy (TEM), scanning transmission electron microscopy (STEM), and scanning electron microscopy (SEM) [5]. The authors herein found that the morphology of C-S-H formed during the hydration of C_3S varies between the early, middle and the late stages of the cement hydration. At the early stages of the hydration, fibrous products were observed on the surface of the grains. During the middle stages, where the rapid exothermic reaction takes place, a mixture of different morphologies was observed. The complete layer of amorphous gel product along the boundaries of the C_3S particle was found while needles with the lengths of 0.75–1.0 μm radiating from the grain and tapered fibers with the length of 0.25–0.5 μm were also observed. In the late stages, the authors found that crumpled foils and dense inner products dominate.

The amorphous, gel-like layer found on the grain at the middle stage of C_3S in Jenning's study above support that the initial reaction products form via heterogenous nucleation and grow outward into water-filled pore solutions. Herein, the rates of nucleation and growth of C-S-H are heavily influenced by the degree of supersaturation of the constituent ions encompassing calcium and silicate ions [4]. It was later found via multiple studies that natural C-S-H found during the PC hydration can be divided into two types showing distinct morphologies. C-S-H gel that occupies the boundary region of the anhydrous cement grain is called an "inner product" and that forms in the originally water-filled pore spaces is called an "outer product." Those two types form at different stages of hydration and exhibit distinct morphologies [6, 7]. Richardson et al. found via TEM analysis that the outer product C-S-H has a fibrillar morphology and that the aspect ratio of the corresponding fibrils depends on the amount of available space in pore spaces [8, 9]. Coarse fibrils with the high aspect ratio were present in larger pore spaces and vice versa. On the other hand, the inner product exhibited a dense, homogeneous morphology with the significantly decreased porosity compared to the outer product (**Figure 1**). Furthermore, within each of the inner and outer type of C-S-H, the size of the anhydrous cement grain also affected the final morphological features [8]. The inner product formed within the smaller cement grains, with each grain being less than around 5 μm, exhibited less density and higher porosity compared to that

http://dx.doi.org/10.5772/intechopen.77723

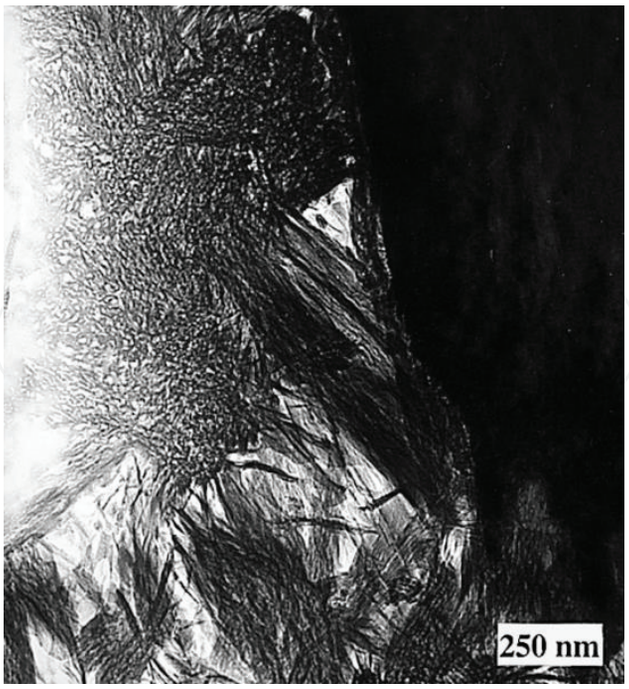

Figure 1. TEM image showing fine, dense morphology of the inner C-S-H and less dense, fibrillary morphology of the outer C-S-H formed during the hydration of C_3S [9].

formed within the larger grains. Richardson et al. further divided the outer product into two morphologically distinct types exhibiting different Ca/Si ratios. The higher Ca/Si ratio corresponded to the fibrillar, directional morphology, while the lower Ca/Si ratio corresponded to the foil-like morphology.

Taylor et al. also found that the age of the sample also significantly affects the morphology of C-S-H found in PC and PC-slag blends [10]. The authors compared the morphology of C-S-H existing in 20-year-old neat PC and PC-slag blend samples with those found in similar samples, which are only 14 months old [10]. The authors found that the outer product found in the 20-year-old neat PC sample is finer, showing little variation in morphology between the inner and the outer product in contrast to the samples, which are 14 months old. Furthermore, the morphology of the outer product C-S-H was different for the PC-slag samples containing different amounts of slag. As the amount of slag was increased from 0 to 90%, the fibrillar morphology was gradually transformed to foil-like morphology and only the crumpled foil was observed for the slag-only paste at the end.

Alkali-silica reaction, which is the common reaction between reactive silica species and alkalis found in cementitious materials, also produces C-S-H with the unique "sheaf of wheat" morphology [11]. Zampini et al. studied the evolution of the wet cement paste-aggregate interface from 5 minutes to 10 days using environmental scanning electron microscopy (ESEM) and found that the C-S-H with a "sheaf of wheat" morphology was formed from the alkali-silica reaction [12]. The authors concluded that formation of this specific morphology is favored at water-to-cement ratio of 0.5, and also facilitated by the inclusion of silica fume. This in turn implies that the presence of silicate ions in a supersaturated solution of hydrated lime is critical in inducing the aforesaid "sheaf of wheat" morphology.

2. Morphology of synthetic C-S-H

Synthetic C-S-H exhibits varying morphologies depending on types of synthesis techniques and experimental factors encompassing the initial Ca/Si ratio and the types of precursors [13, 14]. Common reaction pathways encompass silica-lime reactions, where lime or hydrated lime is reacted with pozzolans such as silica fume and double decomposition technique, where both calcium nitrate and sodium silicate become decomposed into their constituent ions, the ionic building blocks for C-S-H [14–16].

Silica-lime reaction can be performed via either mechanochemical synthesis, where the mixture of silica and lime are reacted in solid state under the assistance of mechanical milling, or solution-based synthesis, where the precursors are reacted in the form of solutions [17–19]. Rodriguez et al. performed the mechanochemical synthesis using lime and fumed silica at different starting Ca/Si ratios, and also carried out the solution-based synthesis using preprepared slurries containing lime and fused silica separately [19]. The authors found that both mechanochemical and solution-based synthesis lead to the formation of foil-like C-S-H regardless of the initial Ca/Si ratio. In contrast, when the authors performed the controlled hydration of pure C_3S at a constant lime concentration, the initial Ca/Si ratio exerted a greater effect on the final morphology. As the Ca/Si ratio was increased from the value below 1.58 to the value above 1.58, the morphology transformed from a foil-like morphology to fiber-like status.

Kurtis et al. synthesized C-S-H via the alkali-silica reaction, where silica sources in the form of the alkali-silicate gel acquired from dam, silica fume and silica gel were reacted with saturated solution of calcium hydroxide. In case of the silica gel, another reaction was performed where it was also exposed to a separate solution of sodium hydroxide and calcium chloride [20]. The authors studied each reaction using high-resolution transmission soft X-ray microscopy and observed

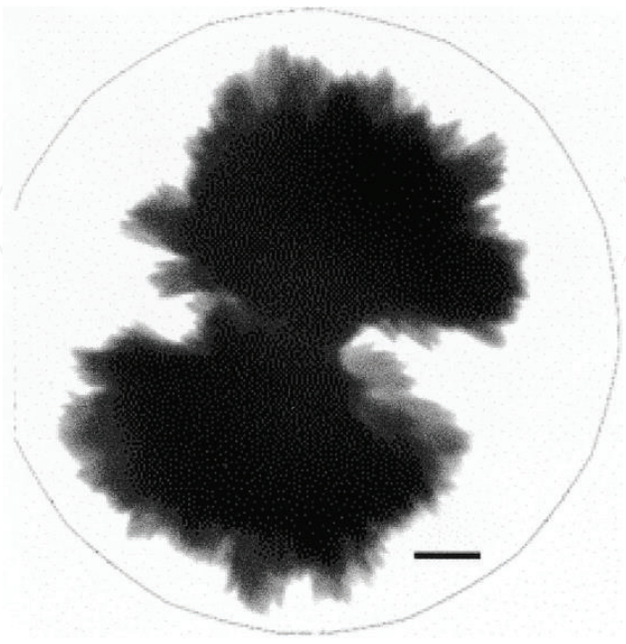

Figure 2. X-ray image showing the "sheaf-of-wheat" morphology for C-S-H acquired from the alkali-silica reaction. Scale bar is 1 μm [36].

the "sheaf of wheat" morphology for the reaction between the alkali-silicate gel and supersaturated solution of calcium hydroxide (**Figure 2**). This implies that the unique "sheaf of wheat" morphology can be materialized by mimicking the natural alkali-silica reaction described above.

3. Formation of crystalline CSH

Hydrothermal synthesis is a common technique used to grow crystalline calcium silicate hydrate phase such as tobermorite $Ca_5Si_6O_{16}(OH)_2{\cdot}4H_2O$, jennite $Ca_9Si_6O_{18}(OH)_6{\cdot}8H_2O$ and xonotlite $Ca_6Si_6O_{17}(OH)_2$, the mineral analogues of amorphous C-S-H from cement hydration. Hara et al. synthesized lath-shaped crystals of jennite, with the width of around 1 μm elongated along b-axis based on hydrothermal reactions of fumed silica and lime at 80°C [13].

During the hydrothermal treatment, addition of metal ions such as sodium and aluminum ions, which are commonly present in supplementary cementitious materials including slag and fly ash, also influences the final type and morphology of crystalline calcium silicate hydrate [21]. Nocuń-Wczelik et al. performed the hydrothermal synthesis using the mixture of metal hydroxide, various powder forms of silica and hydrated lime at the temperature range of 160–240°C. It was shown that sodium and silica content exceeding 20 and 50 wt%, respectively, favor the formation of pectrolyte, the sodium-bearing crystalline product, with broom-like morphology. The addition of aluminum ions to the initial mixture comprising calcium hydroxide, silica and sodium hydroxide facilitated the transformation of amorphous C-S-H to crystalline tobermorite, accompanying the morphological change from the interlocked fibers to plate-like morphology. Furthermore, needle-like xonotlite crystals were formed when the initial Ca/Si ratio was set close to 1 during the hydrothermal synthesis.

Tobermorite, the most commonly referred material for the crystalline analogue of amorphous C-S-H, typically has a basal spacing of 1.1 and 1.4 nm. It can be readily synthesized via the hydrothermal treatment of the ternary $CaO\text{-}SiO_2\text{-}H_2O$ system. 1.1 nm tobermorite is also often observed in hydrothermally cured concretes (tobermorite synthesis under hydrothermal conditions) [22]. Bell et al. performed the hydrothermal treatment of the mixture containing lime and high-purity quartz at the Ca/Si ratio of 0.83 and the pH of 12.6 at 150°C [22]. The reaction led to the formation of two distinct morphologies for tobermorite, platelets and fibers, with the former possibly induced by the heterogenous nucleation and the latter stemming from the homogenous nucleation.

Galvánková et al. studied the effect of different experimental conditions on the formation of tobermorite [23]. Hydrothermal synthesis was performed using the mixture of silica source and grounded limestone, which had been preheated, at the temperature range between 170 and 190°C. Acicular crystals of tobermorite were observed when silica sand was used as the precursor and the reaction temperature beyond 180°C favored the conversion of tobermorite to xonolite.

Hartmann et al. also investigated the effect of the additive Ca-formate on the morphology of crystalline CSH during the hydrothermal reactions [24]. The authors hydrothermally treated the mixture of quartz, lime and calcium formate at 200°C for 40.5 hours and investigated the effect of varying amounts of calcium formate on final morphology of the resultant CSH. The calcium-bearing additive, even with the lowest amount added, induced the morphological

change of tobermorite crystals from typical acicular shape to bent needle-like morphology. This morphological change is likely to have arisen from the adsorption of formate ions on growing (001) faces during the synthesis, thereby impeding the normal growth process of tobermorite. This switches the major growth direction from [001] axis to [010] axis, leading to the observed morphological change.

4. Synthesis of cubic C-S-H and morphology-induced improvement in mechanical properties

The aforesaid control over the morphology of calcium silicate hydrate is somewhat limited to crystalline CSH grown in hydrothermal conditions or amorphous C-S-H with the restricted scope of final shapes encompassing fibrils, plates and foil. Therefore, the extensive control over a wide range of morphologies for gel-like C-S-H had not been accomplished and the range of experimental techniques somewhat lacked diversity. Considering that the surfactant-assisted, template-based synthesis had been widely applied to generate compositionally similar calcium-silicate glass particles with well-defined shapes, the similar techniques could be applied to synthesize C-S-H with a wider range of morphologies than described above [25, 26].

Moghaddam et al. accomplished for the first time the well-defined rhombohedral and cubic morphology for C-S-H, concomitantly proving beneficial properties arising from the specific morphology in the context of construction industry [27]. Herein, the authors employed the surfactant assisted, seed-mediated technique to materialize various well-defined morphologies for C-S-H, where the naturally formed calcium carbonate particles were exploited as seed particles for C-S-H nucleation and growth.

When the silicate source, sodium silicate and calcium source, calcium nitrate were dissolved in water solution under sonication, atmospheric carbon dioxide was also dissolved in the reaction mixture, releasing carbonate ions. The authors hypothesized based on the free energy of formation that in the presence of two types of anions, the silicate and the carbonate ions, calcium ions combine selectively with carbonate ions, thereby forming calcium carbonate seeds [28]. The cationic surfactant, cetyltrimethylammonium bromide (CTAB) stabilized the nanosized seeds, promoting their combination and growth in [104] directions to form microsized seeds with cubic/rhombohedral shapes. Owing to the formation of the seeds described above, the amount of available CO_3^{2-} ions naturally decreased, thereby prompting the subsequent reaction between calcium and silicate ions to form C-S-H. The formation of C-S-H started with the heterogenous nucleation on the microsized $CaCO_3$ seeds as the seed-mediated nucleation is more energetically favorable than homogenous nucleation. The subsequent growth led to the formation of C-S-H with well-defined cubic and rhombohedral morphologies.

Experimental factors such as the initial Ca/Si ratio, temperature of the reaction medium and the types of surfactants all exerted the significant influence on final morphology of the as-formed C-S-H.

Selecting the appropriate type of surfactant was the critical factor for achieving the final well-defined morphology. Cationic surfactants including cetylammonium bromide (CTAB)

could undergo electrostatic interactions with silicate ions and stabilize them, directing the reaction pathway toward the formation of cubic particles. Similarly, tetra(decyl)ammonium bromide (TDAB) ultimately induced a greater variety of morphologies ranging from cubic to rods. In contrast, anionic surfactants such as sodium dodecylsulfate, owing the inherent negative charges, repel the silicate ions and thus could play the stabilizing role similar to CTAB. It is likely that they exerted the undesired electrostatic attraction with calcium ions, disrupting the formation of cubic calcite seeds. Consequently, this led to the formation of highly aggregated, irregularly shaped C-S-H. Also, it was found that using nitrate ions as counterions was the most favorable for the formation of cubic and rhombohedral morphologies, while chloride or hydroxide ions resulted in irregular particles and sheets, respectively.

Aside from the types of surfactants, the final morphology was also influenced by various reaction conditions such as precursor concentration and temperature. An increase in the precursor concentration prompted the formation of larger particles due to the greater availability of ionic building blocks to participate in growth of C-S-H. This also resulted in a greater proportion of twins, triplet and multiplet particles with poorly defined morphologies. On the other hand, when the precursor concentration was low, the as-formed C-S-H seed particles assembled to form dendritic structures instead of serving as the cubic seeds for nucleation and semiepitaxial growth of C-S-H. This hypothesis was verified by the observable cubic subunits, which constitute tails and edges of the dendritic structures under SEM.

The types of counterions within the calcium source also affected the final morphology of C-S-H. The use of calcium nitrate yielded the best results in terms of the cubic/rhombohedral morphology. However, the use of calcium chloride and calcium oxide resulted in C-S-H with poorly defined irregular shapes and crumpled sheets, respectively.

Overall, this sonication-assisted, in situ seed-mediated pathway mapped out the complex, morphology-oriented synthesis of semicrystalline C-S-H using four reaction parameters, encompassing the initial Ca/Si ratio, types of counterions within a calcium source, types of surfactants and the mixing method (**Figure 3**).

The authors then verified the morphology-induced enhancement in mechanical properties based on the combination of nanoindentation technique and compressive testing. Although mechanical properties of synthetic C-S-H have been linked to its final Ca/Si molar ratio or silicate polymerization before, the authors herein proved for the first time the shape-dependent mechanics from the scale of a single particle to assembled states [29, 30]. Compared to the previous reports, where the mechanics of C-S-H had been often evaluated using compacted samples, the authors devised a de novo matrix-based strategy to probe the mechanics of individual C-S-H particles first. The results showed that the individual cubic particles exhibit approximately 650 and 300% increase in hardness and stiffness, respectively, compared to the control C-S-H with irregular morphology. Nanoindentation was also performed on a pressure-induced sample using a (10 × 10) grid, thereby exhibiting ~83 and ~30% increase in the average values of hardness and elastic modulus for cubic samples compared to the control samples, which consisted of irregular C-S-H compacted under external pressure. Furthermore, the compressive toughness and ductility of the cubic samples were ~300 and 77% higher compared to the control samples.

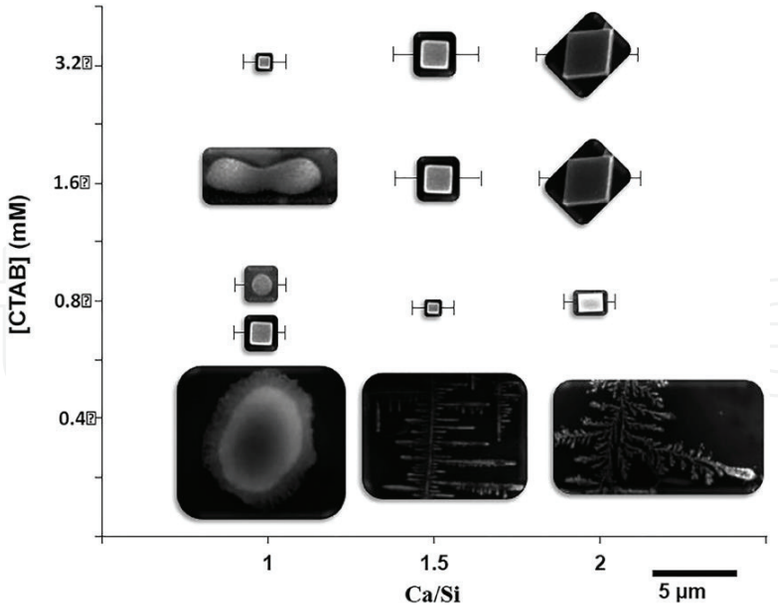

Figure 3. Morphology map as a function of surfactant concentration and the initial Ca/Si molar ratio [27].

5. Morphology of C-S-H for drug delivery

Outside the framework of construction industry, C-S-H also offers numerous benefits as drug carriers, such as high bioactivity and the enhanced affinity toward certain organic drug molecules owing to the presence of calcium ions on the surface [31–33]. Wu et al. synthesized near-spherical, mesoporous C-S-H particles using the surfactant-free, sonochemical method with tetraethylorthosilicate (TEOS) and calcium nitrate as the silicate and calcium source, respectively [33]. Each particle exhibited a 3D-network produced by the assembly of nanosheets, leading to the presence of meso- and macropores (**Figure 4**). The resultant large surface area later facilitated the subsequent loading and unloading of Ibuprofen, utilized as the model drug. Zhang et al. applied the similar sonochemical technique but along with CTAB to produce hollow CSH microspheres [34]. The authors sonicated the mixture of sodium silicate and calcium hydroxide or calcium nitrate, thereby investigating the effect of two distinct calcium-bearing precursors on the final morphology, and also tried two separate mixing techniques, simple stirring and sonication. It was found that well-defined spherical shapes were only produced under sonication while stirring induced the formation of irregular agglomerated nanosheets. Furthermore, calcium hydroxide was found to be a more effective calcium source in inducing hollow spherical morphology than calcium nitrate, owing to the higher dissociation speed of the latter. The fast release of calcium and nitrate ions led to the increased combination rate of calcium and silicate ions prior to the attachment of silicate ions onto the CTAB micelle, thereby resulting in a greater proportion of nonspherical particles. Wu et al. also synthesized ultrathin calcium silicate nanosheets for use as adsorbents for drugs and metal ions [35]. The solvothermal treatment using the as-synthesized nanosheets at 180°C for 24 hours increased crystallinity of the products and induced the nanobelt-like morphology with the thickness of around 5 nm. Further extending this reaction time to 120 hours produced the similar nanobelt-like C-S-H with the enhanced width.

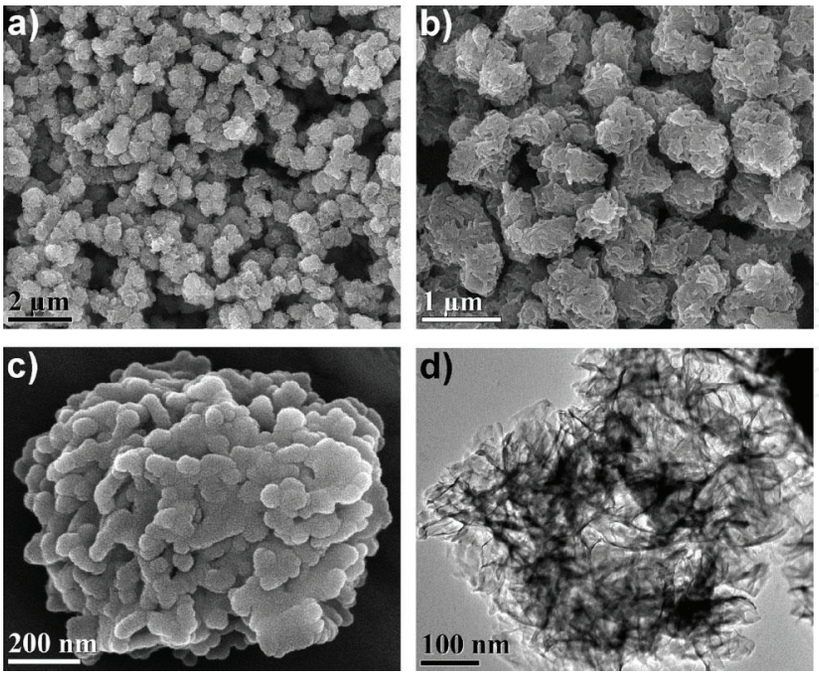

Figure 4. Hierarchically structured, mesoporous C-S-H spheres for drug delivery [33].

6. Conclusion

Calcium silicate hydrate, the most commonly renowned as the glue of concretes, has now found widespread potential applications encompassing cementitious and insulation materials, drug delivery, water treatment and bone-tissue engineering. In addition to the inherent benefits including high strength, high bioactivity and high biodegradability, a long list of various C-S-H members accompanying different stoichiometric ratios implies that there exists a room for the attainment of diverse morphologies. Consequently, a large number of efforts have been directed toward achieving specific, well-defined morphologies, which can optimize the functions. For example, enhanced mechanical properties of cementitious materials arising from cubic building blocks and large drug-loading capacity stemming from the large surface area of mesoporous spherical shapes have been achieved. Based on the rapidly advancing nanofabrication techniques, greater diversity regarding the shapes of C-S-H will be accomplished in future.

Author details

Rouzbeh Shahsavari[1,2,3]* and Sung Hoon Hwang[1]

*Address all correspondence to: rs28@rice.edu

1 Department of Material Science and Nano Engineering, Rice University, Houston, TX, USA

2 Department of Civil and Environmental Engineering, Rice University, Houston, TX, USA

3 The Smalley-Curl Institute, Rice University, Houston, TX, USA

References

[1] Pellenq RJM, Kushima A, Shahsavari R, Van Vliet KJ, Buehler MJ, Yip S, Ulm FJ. A realistic molecular model of cement hydrates. Proceedings of the National Academy of Sciences of the United States. 2009;**106**:16102-16107

[2] Livingston RA. Fractal nucleation and growth model for the hydration of tricalcium silicate. Cement and Concrete Research. 2000;**30**:1853-1860

[3] Thomas JJ. A new approach to modeling the nucleation and growth kinetics of tricalcium silicate hydration. Journal of the American Ceramic Society. 2007;**90**:3282-3288

[4] Valentini L, Favero M, Dalconi MC, Russo V, Ferrari G, Artioli G. Kinetic model of calcium-silicate hydrate nucleation and growth in the presence of PCE superplasticizers. Crystal Growth & Design. 2016;**16**:646-654

[5] Jennings HM, Dalgleish BJ, Pratt PL. Morphological development of hydrating tricalcium silicate as examined by electron-microscopy techniques. Journal of the American Ceramic Society. 1981;**64**:567-572

[6] Diamond S. The microstructure of cement paste and concrete-A visual primer. Cement and Concrete Composites. 2004;**26**:919-933

[7] Taylor HFW. Cement Chemistry. 2nd ed. Thomas Telford; 1997

[8] Richardson IG. The nature of C-S-H in hardened cements. Cement and Concrete Research. 1999;**29**:1131-1147

[9] Richardson IG. The nature of the hydration products in hardened cement pastes. Cement and Concrete Composites. 2000;**22**:97-113

[10] Taylor R, Richardson IG, Brydson RMD. Composition and microstructure of 20-year-old ordinary Portland cement-ground granulated blast-furnace slag blends containing 0 to 100% slag. Cement and Concrete Research. 2010;**40**:971-983

[11] Wang H, Gillott JE. Mechanism of alkali-silica reaction and the significance of calcium hydroxide. Cement and Concrete Research. 1991;**21**:647-654

[12] Zampini D, Shah SP, Jennings HM. Early age microstructure of the paste-aggregate interface and its evolution. Journal of Materials Research. 1998;**13**:1888-1898

[13] Hara N, Inoue N. Formation of jennite from fumed silica. Cement and Concrete Research. 1980;**10**:677-682

[14] Chen JJ, Thomas JJ, Taylor HFW, Jennings HM. Solubility and structure of calcium silicate hydrate. Cement and Concrete Research. 2004;**34**:1499-1519

[15] Shi CJ, Day RL. Pozzolanic reaction in the presence of chemical activators-Part I. Reaction kinetics. Cement and Concrete Research. 2000;**30**:51-58

[16] Shi CJ, Day RL. Pozzolanic reaction in the presence of chemical activators-Part II. Reaction products and mechanism. Cement and Concrete Research. 2000;**30**:607-613

[17] Saito F, Mi GM, Hanada M. Mechanochemical synthesis of hydrated calcium silicates by room temperature grinding. Solid State Ionics. 1997;**101**:37-43

[18] Sasaki K, Masuda T, Ishida H, Mitsuda T. Synthesis of calcium silicate hydrate with Ca/Si=2 by mechanochemical treatment. Journal of the American Ceramic Society. 1997;**80**: 472-476

[19] Rodriguez ET, Richardson IG, Black L, Boehm-Courjault E, Nonat A, Skibsted J. Composition, silicate anion structure and morphology of calcium silicate hydrates (C-S-H) synthesised by silica-lime reaction and by controlled hydration of tricalcium silicate (C3S). Advances in Applied Ceramics. 2015;**114**:362-371

[20] Kurtis KE, Monteiro PJM, Brown JT, Meyer-Ilse W. High resolution transmission soft X-ray microscopy of deterioration products developed in large concrete dams. Journal of Microscopy (Oxford). 1999;**196**:288-298

[21] Nocun-Wczelik W. Effect of Na and Al on the phase composition and morphology of autoclaved calcium silicate hydrates. Cement and Concrete Research. 1999;**29**:1759-1767

[22] Bell NS, Venigalla S, Gill PM, Adair JH. Morphological forms of tobermorite in hydrothermally treated calcium silicate hydrate gels. Journal of the American Ceramic Society. 1996;**79**:2175-2178

[23] Galvánková L, Másilko J, Solný T, Štěpánková E. Tobermorite synthesis under hydrothermal conditions. Procedia Engineering. 2016;**151**:100-107

[24] Hartmann A, Khakhutov M, Buhl JC. Hydrothermal synthesis of CSH-phases (tobermorite) under influence of Ca-formate. Materials Research Bulletin. 2014;**51**:389-396

[25] Hwang SH, Miller JB, Shahsavari R. Biomimetic, strong, tough, and self-healing composites using universal sealant-loaded, porous building blocks. ACS Applied Materials & Interfaces. 2017;**9**:37055-37063

[26] Li X, Zhang LX, Dong XP, Liang J, Shi JL. Preparation of mesoporous calcium doped silica spheres with narrow size dispersion and their drug loading and degradation behavior. Microporous and Mesoporous Materials. 2007;**102**:151-158

[27] Moghaddam SE, Hejazi V, Hwang SH, Sreenivasan S, Miller J, Shi BH, Zhao S, Rusakova I, Alizadeh AR, Whitmire KH, Shahsavari R. Morphogenesis of cement hydrate. Journal of Materials Chemistry A. 2017;**5**:3798-3811

[28] Rog G, Kozlowskarog A. Determination of the standard Gibbs free-energies of formation of the calcium silicates by Emf-measurements. The Journal of Chemical Thermodynamics. 1983;**15**:107-110

[29] Kim JJ, Foley EM, Taha MMR. Nano-mechanical characterization of synthetic calcium-silicate-hydrate (C-S-H) with varying CaO/SiO_2 mixture ratios. Cement and Concrete Composites. 2013;**36**:65-70

[30] Pelisser F, Gleize PJP, Mikowski A. Effect of the Ca/Si molar ratio on the micro/nano-mechanical properties of synthetic C-S-H measured by nanoindentation. Journal of Physical Chemistry C. 2012;**116**:17219-17227

[31] Hench LL. Bioceramics. Journal of the American Ceramic Society. 1998;**81**:1705-1728

[32] Coleman NJ, Bellantone M, Nicholson JW, Mendham AP. Textural and structural properties of bioactive glasses in the system CaO-SiO_2. Ceramics-Silikáty. 2007;**51**:1-8

[33] Wu J, Zhu YJ, Cao SW, Chen F. Hierachically nanostructured mesoporous spheres of calcium silicate hydrate: Surfactant-free sonochemical synthesis and drug-delivery system with ultrahigh drug-loading capacity. Advanced Materials. 2010;**22**:749

[34] Zhang ML, Chang J. Surfactant-assisted sonochemical synthesis of hollow calcium silicate hydrate (CSH) microspheres for drug delivery. Ultrasonics Sonochemistry. 2010;**17**: 789-792

[35] Wu J, Zhu YJ, Chen F. Ultrathin calcium silicate hydrate nanosheets with large specific surface areas: Synthesis, crystallization, layered self-assembly and applications as excellent adsorbents for drug, protein, and metal ions. Small. 2013;**9**:2911-2925

[36] Gartner EM, Kurtis KE, Monteiro PJM. Proposed mechanism of C-S-H growth tested by soft X-ray microscopy. Cement and Concrete Research. 2000;**30**:817-822